International Journal of Engineering & Technology, 7 (3.27) (2018) 593-600

International Journal of Engineering & Technology

Website: www.sciencepubco.com/index.php/IJET

Research paper

Classification of Textures based on Circular and Elliptical Weighted Symmetric Texture Matrix

J.Srinivas[1], Ahmed Abdul Moiz Qyser[2], B. Eswara Reddy[3]

[1]Research Scholar at JNTUA, Ananthapuramu, India
Associate Professor, Muffakham Jah College of Engineering and Technology, Hyderabad, India
Email: Jagirdar.srinivas@gmail.com•
[2]Department of CSE, Muffakham Jah College of Engineering and Technology, Hyderabad, India
Email: aamoiz@mjcollege.ac.in
[3]Principal, JNTUA College of Engineering, Kalikiri – Chittoor Dist.Andhra Pradesh, India
**Corresponding author E-mail: eswarcsejntua@gmail.com*

Abstract

The Local binary patterns (LBP) derive most efficient high-performance texture features. However, the LBP method derives only isotropic structural features and is unable to capture anisotropic structural information. The elliptical LBP(ELBP) captures only anisotropic information. The LBP, ELBP and its variants derives a wide range of histograms and thus not suitable to integrate second order statistics. To best address this disadvantage, in this paper, we introduce novel descriptors for texture classification, the circular and elliptical weighted symmetric texture matrix (CEWSTM) and robust CEWSTM (RCEWSTM). Different from the traditional LBP, many LBP variants and ELBP, CEWSTM derives a weighted symmetric relationship among the sampling points of circular and elliptical neighborhood (CEN).The CEWSTM computes a texture matrix by efficiently deriving a co-occurrence matrix and its features on weighted center symmetric codes of CEN which can capture microstructure texture information of isotropic and anisotropic structurers. A comprehensive evaluation on benchmark data sets reveals CEWSTM's high performance, robust to gray scale variations, rotation changes but at a low computational cost.

Keywords: *Texture descriptors, rotation invariance, isotropic and anisotropic structures.*

1. Introduction

TEXTURE is the significant representative of many types of images, ranging from large-scale multispectral remotely sensed data to microscopy. And one of the major and crucial issues of texture analysis is the texture classification. The texture classification is considered to be one of the major and long standing research topics due to its importance of its role in the wide variety of applications of computer vision and image analysis [1], [2]. Texture classification plays a vital role in many important applications like object recognition, biometrics, image retrieval, document classification, face recognition, age classification, remote sensing, medical image analysis and understanding. Texture classification basically consists of two sub problems. The first one is the feature extraction and the second one is the classifier designation. Derivation of powerful features plays an important and vital role in texture classification than classifier selection. The selection of poor features under a best classifier, will fail in achieving the good results. That's why the research in texture classification mainly concentrated on extraction of best features. In the literature various texture feature extraction methods are developed [3-5]; however these methods are not suitable to real time applications, due to their dimensionality and time consuming process, and also they demand the data base size, environment in which images are captured etc.. the most important goal for a researcher in texture classification field is to derive powerful and significant features that balances the two competing goals: derivation of high quality descriptors and computational complexity. The high quality recognition is sometimes achieved by integrating several types of features. The high quality descriptors of texture classification should consider the large intra class variations of textures, environment and factors of variations like illumination, scale, rotation, noise, blur, and occlusion etc..,

The recent texture feature descriptor Local Binary Patterns (LBP) [6] proposed by ojala et el, emerged as most significant and prominent texture descriptor and attracted many researchers working in the field of computer vision and image analysis. This is mainly because LBP is very easy to understand and implement ; low computational complexity and invariance to monotonic illumination. Though LBP is initially derived for texture analysis, today LBP is extensively used in many applications [7--11].

To improve further the efficiency, discriminative power, and robustness of LBP, many variants or extensions to LBP are proposed in the literature and they are widely used for many applications in the field of pattern recognition, computer vision and image processing. The LBP variants like: Local Ternary Patterns(LTP)[12], Discriminative Completed Local Binary Pattern (disCLBP) [13], Extended Local Binary Pattern (ELBP) [14], Completed Local Binary Pattern (CLBP) [15], Pairwise Rotation Invariant Co-occurrence Local Binary Pattern (PRICoLBP) [16] and the combination of Dominant Local Binary Pattern (DLBP) and Gabor filtering features [17] are proposed in the literature to improve the discriminativeness and efficiency. The above LBP variants though they are efficient and discriminate, however they have no or min-

imum tolerance to blur, noise and the main disadvantage is their high dimensionality, which makes them not suitable to real time applications. To overcome the image degradation due to noise various LBP variants are proposed in the literature like: Local Phase Quantization (LPQ) [18],Local Ternary Pattern (LTP) [12], Fuzzy Local Binary Pattern (FLBP) [19], Robust Local Binary Pattern (RLBP) [20] Median Binary Pattern (MBP) [21], Noise Tolerant Local Binary Pattern (NTLBP) [22] and Noise Resistant Local Binary Pattern (NRLBP) [23]; however most of them yield high dimensionality and sometimes the noise tolerance capability of these methods remains unsatisfactory.

The local texture classification and analysis algorithms have shown better performance than holistic or global approaches [24, 25, 26]. The global approaches are sensitive to complicated changes like illumination, noise, local contrast etc… The local neighbourhood based methods are simpler, robust under varying challenging conditions like illumination variations, noise, rotation variation and further they are simple to implement, understand and they can be integrated with many other structural and statistical methods. The local feature based methods have become more and more popular by the derivation of Local Binary Pattern (LBP). The LBP variants achieved its success due to its precise and accurate representation of local features. The LBP and its variants played a vital role and achieved a high accuracy, recognition rate in many applications related texture classification and analysis: image retrieval [27-29],shape localization [30], face recognition [31, 32],background modelling and detection using LBP [33], emotion estimation [34, 35], interest region description [36], texture segmentation [37] and rotational invariant texture classification [8]..

2. Related Work

2.1 Local Binary Pattern

The relationship between centre pixel of the neighbourhood with its neighbouring pixels defined the basic LBP descriptor. This relationship assigns a value 1 or 0 to the neighbouring pixels as given in equation 1. Using this binary relationship The LBP derives a unique LBP code using the equation 1 and 2.

$$LBP_{P,R} = \sum_{i=1}^{P} 2^{(i-1)} * f_1(I(v_i).I(v_c)) \quad (1)$$

$$f_1(x) = \begin{cases} 1 \text{ if } x \geq 0 \\ 0 \text{ otherwise} \end{cases} \quad (2)$$

Where: P represents the number of neighbouring pixel surrounded over the central pixel, R represents the radius of the neighbourhood, I(v_i) and I(v_c) are the gray level invariant values of the neighbouring pixel i and centre pixel c respectively. The LBP is extended with more number of sampling points 'p' with different radius 'R'.

Elliptical LBP (ELBP)

The LBP which is derived only on circular neighbourhood accomplishes rotational invariance; however it holds only local isotropic structural features. For a more precise and accurate local features one should also consider the anisotropic structural information. The anisotropic information can be obtained by considering the elliptical neighbourhood (EN), instead of a circular neighbourhood (CN). In the literature only very few authors worked on EN and derived Elliptical local Binary Pattern (ELBP). The Following Fig.1 displays the circular and elliptical neighbourhoods. The complete anisotropic information is captured from two types of EN: horizontal-EN(H-EN) and vertical-EN(V-EN) as shown in Fig 1. All the three basic neighbourhoods: i) CN ii) H-EN iii) V-EN have 8-sampling points surrounded by the centre pixel Pc.

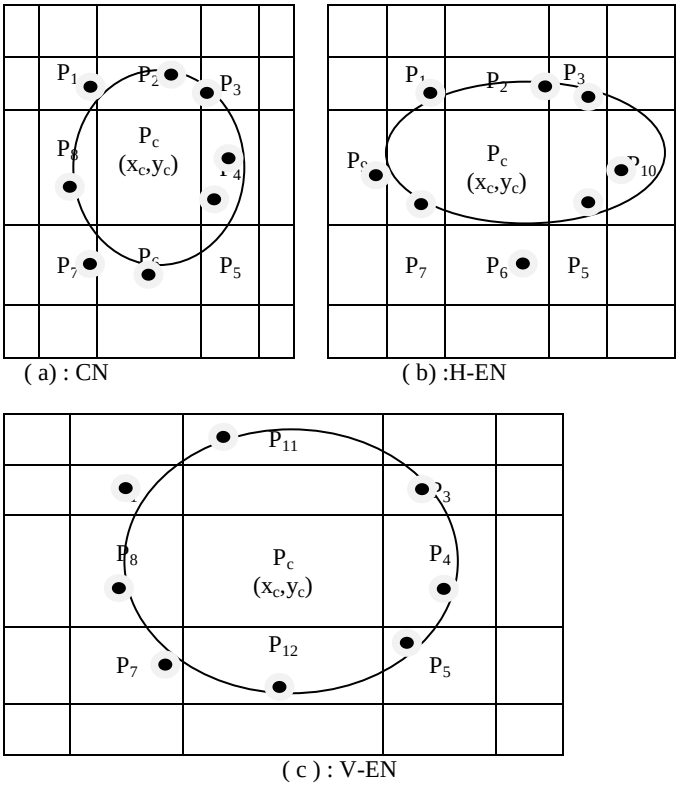

(a) : CN (b) :H-EN

(c) : V-EN

Fig: 1: The representation of basic CN,H-EN, V-EN.

The basic disadvantage in capturing complete anisotropic information is one should consider two special types of elliptical neighbourhoods and this increases overall complexity and this is the main reason for not considering the EN over CN in the literature. In literature Horizontal Elliptical LBP (H-ELBP) and vertical- Elliptical LBP(V-ELBP) are derived in the same manner as LBP.

To derive an ellipse on an EN , one need to have three parameters i.e., i) vertical (y-axis) radius of ellipse ii) horizontal (X-axis) radius iii) the number of sampling points. The vertical (y-axis) radius, horizontal (X-axis) radius and the number of sampling points are denoted by HR, VR and P respectively. The horizontal Ellipse (HE) and vertical ellipse (VE) are derived based on the relationship between HR and VR of EN. The LBP derived on HE and VE are known as H-ELBP and V-ELBP respectively and each of them represents the partial anisotropic local structural information. To derive the complete anisotropic local information precisely and accurately one should combine or concatenate the features derived from H-ELBP and V-ELBP. Further in ELBP the sampling pixel (xi,yj) around the centre pixel (xc,yc) is derived, based on the following equations that represent basic ellipse.

$$\mathbf{a}\text{ngle} - \text{step} = 2 * \frac{\pi}{n} \quad (3)$$

$$X_i = x_c + HR * (\cos(i-1) * \text{angle} - \text{step}) \quad (4)$$

$$Y_j = Y_c + VR * (\cos(i-1) * \text{angle} - \text{step}) \quad (5)$$

If HR = VR, then ELBP becomes LBP, HR > VR, then ELBP represents H-ELBP otherwise when HR < VR the ELBP becomes V-ELBP. The ELBP is denoted as ELBPP,HR,VR. The unique decimal code for ⟦ H-ELBP⟧ ^(P,HR,VR) (x_c,y_c)and V-ELBPP,HR,VR (xc,yc) at each centre pixel (xc,yc) is derived just like LBP based on equation 6 and 7.

$$\mathbf{ELBP^{P,HR,VR}(x_c, y_c)} = \sum_{i=1}^{P} \mathbf{s\left(P_i^{n,HRVR} - P_c\right).2^{i-1}} \quad (6)$$

Where S(x) is defined as

$$S(x) = f(x) = \begin{cases} 1, & \text{if } x \geq 0 \\ 0, & x < 0 \end{cases} \quad (7)$$

The decimal codes of conventional LBP8,1, H-ELBP8,2,1 and V-ELBP8,2,1 ranges from 0 to 2d-1 (255). The LBP or H-ELBP or V-ELBP descriptor transforms the image into LBP or H-ELBP or V-ELBP coded image by deriving respective code on the given window and replaces the central pixel value with the respective code. And this process is continued on the entire image with a step length of one. This transforms the grey level image into respective (LBP or H-ELBP or V-ELBP) coded image. The LBP, ELBP (both horizontal and vertical), are invariant to monotonic grey level brightness changes. Hence, they are robust to brightness and contrast dissimilarities. A histogram can be derived based on these codes as given in equation 8.

$$H_{LBP}^{(I)} = \sum_{r}^{r_n} \sum_{c}^{c_n} f_2\,(LBP(r,c), l); \quad l \in [0, (2^P - 1)] \quad (8)$$

$$f_2(x,y) = \begin{cases} 1, & x = y \\ 0, & \text{else} \end{cases} \quad (9)$$

where the size of the LBP or H-ELBP or V-ELBP coded image is $r_n * c_n$.

3. Methodology

The capture complete anisotropic information more precisely one should consider the both H-ELBP and V-ELBP. The H-ELBP and V-ELBP requires 12-sampling points and out of which the diagonal points P1, P3, P5, P6 are common (Fig. 1). The H-ELBP and V-ELBP produces a histogram of basic size 256 each, which is very huge. To address this following strategy can be adopted:

i) Derivation of complete histogram by considering all the 12-sampling points and in this case the histogram ranges from 0 to 212-1, which is very huge.

ii) To address the above problem of i) one can derive a single histogram by concatenating the both H-ELBP and V-ELBP. In this case the histogram size will range from 0 to 511, which is also huge.

iii) The histogram methods are not resulted a good classification rate and that's why the local based methods are integrated mostly with other operators or descriptors. The best results are obtained when local descriptors are integrated with grey level co-occurrence features. For this on has derive GLCM on the local descriptors. If the GLCM is derived using the 12-sampling points of both H-ELBP and V-ELBP and in this case the dimension of the H-V-ELBP-GLCM ranges from 212-1 x 212-1, which is very huge. Otherwise one can derive two individual GLCMs on H-ELBP and V-ELBP coded image and the average features of these two can be used for classification. In this case the dimension of each matrix will be (H-ELBP-GLCM or V-ELBP-GLCM) 256 x 256.

From the Fig. 1 it is noted that 12-sampling points are required to represent the three neighbourhoods i.e. i) CN ii) H-EN iii) V-EN and respective local binary patterns can be derived from this. The following Fig. 2 represents the sampling points that are required for these three LBP's.

		P_{11}		
	P_1	P_2	P_3	
P_9	P_8	P_c	P_4	P_{10}
	P_7	P_6	P_5	
		P_{12}		

Fig. 2: The sampling points of H-ELBP; V-ELBP and LBP (Circular LBP).

Out of these (P1,P2…., P7, P8) are the 8-sampling points of LBP and P9 and P10 are the additional sampling points required for H-ELBP and P11 and P12 are for V-ELBP. The diagonal pixels of LBP P1, P3, P5 and P7 are common among the three local patterns i.e. the LBP, H-ELBP and V-ELBP. The neighbourhood pixels of LBP (P2 , P6) and (P4 , P8)are common among LBP and H-ELBP and LBP and V-ELBP respectively.

To achieve a better accuracy in texture classification and analysis one should consider both isotropic and anisotropic information and features. To derive complete local isotropic and anisotropic structural information one should consider the features derived from the three LBPS i.e.: H-ELBP, V-ELBP and LBP. In this case, the number of bins of histogram ranges from 0 to 767 which increase the dimensionality to a huge extent. To overcome this dimensionality problem and to capture both isotropic and anisotropic structural information, one or two methods are proposed in the literature.

1. In the literature recently Circular and Elliptical LBP(CE-LBP) [38] is derived by quantizing the 12- common sampling points of LBP, H-ELBP and V-ELBP in to 8 and also quantized the neighbourhood in to 3 x 3 as shown in Fig. 3.

P_1	$(P_2+ P_{12})/2$	P_3
$(P_8+ P_9)/2$	P_c	$(P_4+ P_{10})/2$
P_7	$(P_6 +P_{11})/2$	P_5

Fig. 3: The quantized sampling points of CE-LBP.

The CE-LBP reduces overall code to 28 from 212-1 by preserving the overall anisotropic and isotropic information. To derive GLCM features, the CE-LBP derives a huge matrix of size 256 x 256.

2. To address the above disadvantage of high dimensionality of CE-LBP authors derived cross diagonal- circular and Elliptical texture matrix (CD-CETM)[39] by dividing the CE-LBP in to two units with four pixels each. The CD-CETM extracted cross circular and Elliptic patterns (C-CEP) and diagonal circular and Elliptic patterns (D-CEP) by deriving a relationship between centre pixel with cross and diagonal pixels as given in equation 12 and 13. A unique code for cross and diagonal circular and elliptical neighbourhood is generated from the above equations and it ranges from 0 to 80 (0 to 34-1). The CD-CETM elements has relative frequencies of cross and diagonal circular and elliptical codes and the code values are placed on x and y axis respectively. The CD-CETM has a "fixed size of 81x81. Also the grey level of the image has no effect on the size of the matrix as in GLCM. In addition, the computational time complexity is reduced.

$$c_i(d_i) = \begin{cases} 2\ c_i(p_i) > p_c \\ 1\ c_i(P_i) = p_c \\ 0\ c_i(P_i) < p_c \end{cases} \quad \text{where i= 1,2,3,4} \quad (10)$$

$$CCEP_c(v_c) = \sum_{i=1}^{4} 3^{i-1} * c_i \quad (11)$$

$$DCEP_c(v_c) = \sum_{i=1}^{4} 3^{i-1} * d_i \quad (12)$$

The above CE-LBP and CD-CETM approaches captures both isotropic and anisotropic information; however the quantization mechanism of CE-LBP may lose some information and further it derives a GLCM of size 256 x 256 and Cd-CETM reduces the

dimensionality to 81 x 81. This paper proposes a new scheme based on the centre symmetric relationship of neighbouring pixels, to derive more significant information from CN and EN with low dimensionality. In the literature, centre symmetric LBP (CS-LBP) [40] is proposed and it derives 4-bit code based on the relationship between centre symmetric in surrounding pixels based on the following equation.

$$CS-LBP = \sum_{i=1}^{4} 2^{i-1} * f_1(I(P_i) - I(P_{i+4})) \quad (13)$$

$$f(x) = \begin{cases} 1, & x \geq 0 \\ 0, & \text{otherwise} \end{cases} \quad (14)$$

The CS-LBP reduces the LBP code range from2^(p) to 2^4. Thus the CS-LBP reduces the overall dimensionality of LBP and thus more suitable to integrate with statistical models like GLCM. However the main disadvantages of CS-LBP are

1. It does not consider centre pixel while deriving the relationship between symmetric neighbouring pixels. Thus it loses the overall concept of basic LBP.
2. It derives only isotropic or circular neighbourhood local features.
3. It generates only a 4-bit code, thus does not hold the significant information.

This paper extracts complete local information from the circular and elliptical neighbourhood by deriving circular and Elliptical weighted Symmetric LBP (CE-WS-LBP). The CE-WS-LBP descriptor captures the complete isotropic and anisotropic information by considering the centre pixel. The CE-WS-LBP derives a 6 bit code as given in the equation.

$$CE-WS-LBP_{P,R} = 2^0 * f_1((I(P_1) + I(P_5) - 2 * I(P_c)) + 2^1 * f_1((I(P_2) + I(P_6) - 2 * I(P_c)) + 2^2 * f_1((I(P_3) + I(P_7) - 2 * I(P_c)) + 2^3 * f_1((I(P_4) + I(P_8) - 2 * I(P_c)) + 2^4 * f_1((I(P_{11}) + I(P_{12}) - 2 * I(P_c)) + 2^5 * f_1((I(P_9) + I(P_{10}) - 2 * I(P_c)) \quad (15)$$

$$f(x) = \begin{cases} 1, & x \geq 0 \\ 0, & \text{otherwise} \end{cases} \quad (16)$$

The following figure four illustrates the relationship between LBP, CS-LBP and the proposed CE-WS-LBP. The proposed CE-WS-LBP holds more precise and significant information about circular and elliptical symmetrical information. The advantage of the proposed approach is it derives binary pattern based on weighted central pixel value.

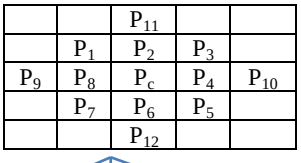

LBP	CS-LBP	CE-WS-LBP
$s(P_1-P_c)*2^0 + s(P_2-P_c)*2^1 + s(P_3-P_c)*2^2 + s(P_4-P_c)*2^3 + s(P_5-P_c)*2^4 + s(P_6-P_c)*2^5 + s(P_7-P_c)*2^6 + s(P_8-P_c)*2^7$	$s(P_1-P_5)*2^0 + s(P_2-P_8)*2^1 + s(P_3-P_7)*2^2 + s(P_4-P_8)*2^3$	$2^0*f_1((I(P_1)+I(P_5)-2*I(P_c)) + 2^1* f1(I(P_2)+I(P_6)-2*I(Pc)) + 2^2* f1(I(P_3)+I(P_7)-2*I(Pc)) + 2^3* f1(I(P_4)+I(P_8)-2*I(Pc)) + 2^4* f1(I(P_{11})+I(P_{12})-2*I(Pc)) + 2^5* f1(I(P_9)+I(P_{10})-2*I(Pc))$

Fig. 4: Relationship between LBP, CS-LBP and proposed CE-WS-LBP features.

This paper also derives another extension for the proposed CE-WS-LBP. The new descriptor maps the CE-WS-LBP code and its complement to the minimum of the two. For example the complement for the CE-WS-LBP code 110010 will be 001101; the states are changed from 0 to 1 or1 to 0 during this mapping. The minimum of these codes min { 110010, 001101} will be 001101. The new descriptor is named as Robust CE-WS-LBP (CE-RWS-LBP). And CE-RWS-LBP code will be the minimum of the above mapping. By this the RWS-LBP code becomes the reversal of intensity between the back ground and the objects and further the range of the code becomes half i.e. in this case 26 /2. RWS-LBP is computed as follows:

$$CE\text{-}RWS\text{-}LBP_{P,R} = \min\{ CE\text{-}WS\text{-}LBP_{P,R}, ((2^N - 1) - CE\text{-}WS\text{-}LBP_{P,R}) \}, \quad (17)$$

Where N is the number of summation terms of CE-WS-LBPP,R as defined in Eq (17) and ((2N−1)−CE-WS-LBPP,R) is the complement code of CE-WS-LBPP,R. The advantage of this mapping is it halves the number of CE-WS-LBP P,R codes, the CE-RWS-LBP P,R bin number is 32 for N= 6.

		20		
	42	58	65	
16	56	23	48	21
	62	35	45	
		15		

(a) CE_LBP neighborhood

111100
Code=15

(b) CE-WS-LBP code

000011
Code= 48

(c) CE-RWS-LBP - code

Fig 5: (a)The basic Circular and elliptical neighbourhood window (b) The generation of CE-WS-LBP and its code (c) The CE-RWS-LBP code.

This paper initially transforms the given image into grey level image, and transforms the grey level image in to CE-WS-LBP coded image by convolving the entire image with a step length of one. The derived CE-WS-LBP code replaces the centre pixel value. In the similar way, this paper transforms the given texture image into CE-RWS-LBP coded image. This paper constructs grey level co-occurrence matrix (GLCM) on the CE-WS-LBP coded image and also on CE-RWS-LBP coded image and this results a circular and elliptical weighted symmetric Texture matrix (CEWSTM) and Robust circular and elliptical weighted symmetric Texture matrix (RCEWSTM). The dimension of the CEWSTM and RCEWSTM will be 64 x 64 and 32 x 32 respectively. The GLCM is one of the oldest and still popular and benchmark proposed by Haralick [41] and it is widely used and integrated with many other models due to its high classification rate. This paper derives five GLCM features as given below:

1. Contrast :

$$Contrast = \sum_{n=0}^{M-1} n^2 \left\{ \sum_{i=1}^{M} \sum_{j=1}^{N} X(i,j) \right\}, |i-j| = n \quad (18)$$

This measure of contrast or local intensity variation will favor contributions from P (i, j) away from the diagonal, i.e. i ! = j.

1. Correlation :

$$Correlation = \sum_{i=0}^{M-1} \sum_{j=0}^{N-1} \frac{\{iXj\}XX(i,j) - \{\mu_x X \mu_y\}}{\sigma_x X \sigma_y} \quad (19)$$

Correlation is a measure of grey level linear dependence between the pixels at the specified positions relative to each other.

2. Entropy :

$$Entropy = \sum_{i,j} \log(X(i,j)).\ X(i,j) \quad (20)$$

Inhomogeneous scenes have low first order entropy, while a homogeneous scene has high entropy.

3. Homogeniety, Angular Second Moment (ASM):

$$ASM= \sum_{i=0}^{G-1} \sum_{j=0}^{G-1} \{X(i,j)\}^2 \quad (21)$$

ASM is a measure of homogeneity of an image. A homogeneous scene will contain only a few grey levels, giving a GLCM with only a few but relatively high values of P (i, j). Thus, the sum of squares will be high.

5. Local Homogeneity, Inverse Difference Moment (IDM)

$$IDM= \sum_{i=0}^{G-1} \sum_{j=0}^{G-1} \frac{1}{1+(i-j)^2} P(i,j) \quad (22)$$

IDM is also influenced by the homogeneity of the image. Because of the weighting factor (1+(i−j)2)−1 IDM will get small contributions from inhomogeneous areas (i != j). The result is a low IDM value for inhomogeneous images, and a relatively higher value for homogeneous images.

4. Results and Discussions

To evaluate the performance, this paper compared the classification rates with various other LBP based descriptors i.e. LBP[6], ULBP[42], LTP[12], CS-LBP[40] and CLBP-SMC[43]. The experiments are conducted on five different popular data bases namely, Brodtaz [44], UIUC[45], Outex-TC-12[46], KTH-TIPS [47] and A LOT[48]. A brief description about these databases is given below.

A. Brodtaz Data base:

Thirty different images of 640 x 640 dimensions are selected from Brodtaz texture data base and sample images are displayed in Fig. 6. For classification purpose each image is divided in to a size of 128 x 128. This division is carried out in a non-overlapped manner. This mechanism results 25 images for each class and this results a total of 30 x 25=750 images of Brodtaz database. The proposed classifiers were trained by using 10 samples of each class (30 x 10=300 images in total) of Brodtaz database and the remaining 15 samples per class were used for validation (30 x 15=450 images in total).

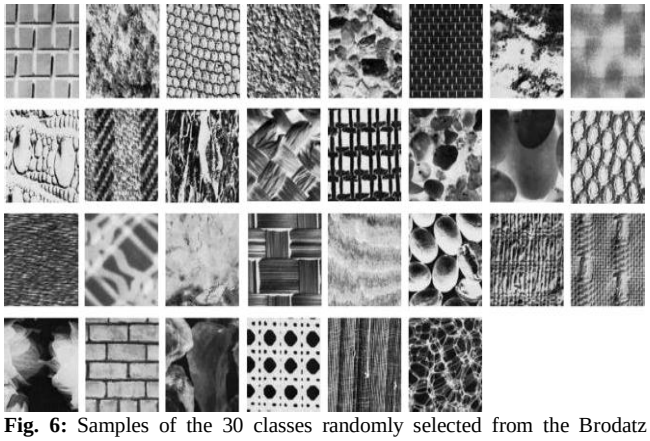

Fig. 6: Samples of the 30 classes randomly selected from the Brodatz database.

B. UIUC Data base

The sample images of UIUC database are shown in Fig. 7. The UIUC database consists of 25 different classes of real time textures. And each class consists of 40 images. Each texture image of UIUC database is of 640 x 480 pixels. The UIUC database consists of 1000 textures i.e.25 different classes and 40 images per class. This paper divided each image into a size if 128 x 128 in a non-overlapped manner. That is each image is divided into 15 images. Thus this paper extended the UIUC database with 15000 images i.e. 25 x 40 x 15. And each class of texture consists of 40 x 15=600 images. This paper considered 200 images from each class as training purpose (40 x 5=200) and the remaining 400 textures from each class are considered for testing purpose.

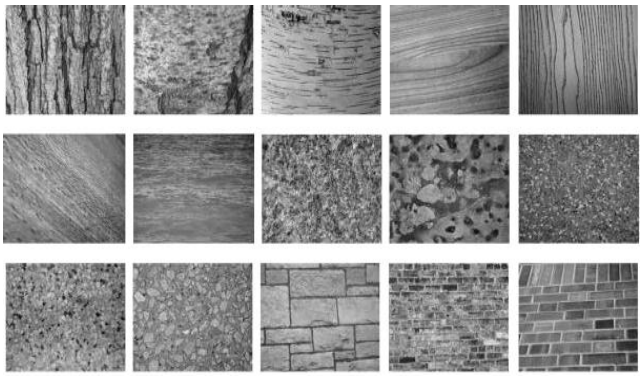

Fig. 7: Sample images from the UIUC database.

C. Outex-TC-12 database

The Outex database contains two test suits: Outex-TC-10(TC12-000) and Outex-TC-12(TC12-001). This paper considered the test suite TC12 (also known as Outex_TC_00012) for texture classification. The TC12 texture images are captured under different rotation angles i.e. 0°, 5°, 10°, 15°, 30°, 45°, 60°, 75°,and 90° . There are 20 images under each rotation angle and the TC12 consists of 24 texture classes with a resolution of 128 x 128. These images are captured under three illumination conditions namely 1. "inca' 2. t184 3.Horizon.There are 480 images in TC12 under inca in a single direction (24 x 20=480). There are 4320 t184 images and 4320 horizon images in TC12 under nine rotation angles (24 x 20 x 9=4320). This leads to a total of 9120 images in TC12. This paper considered illumination "inca" with zero degree rotation texture images for training purpose (24 x 20=480 images). The 4320 (24 x 20 x9) sample texture images captured under illumination tl84 and horizon with 9 different orientations are used as test data. The sample images from Outex database are shown in Fig.8.

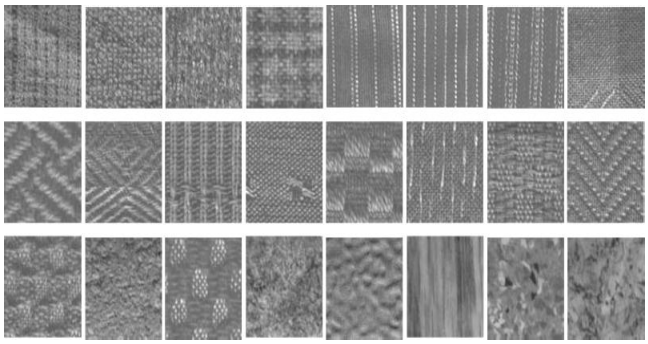

Fig.8: The sample images of 24 classes from Outex database.

D. KTH-TIPS database

This paper considered 10 different classes of texture images from KTH-TIPS data base shown [47] . The KTH-TIPS (Textures under varying Illumination, Pose and Scale) image database was created to extend the CUReT database in two directions, by providing variations in scale as well as pose and illumination, and by imaging other samples of a subset of its materials in different settings. And each class consists of 81 textures images (10 x 81=810total images). This paper treats these images as a stand-alone dataset [47] . This paper considered 30 texture images from each sample for training propose (10x 30=300) and the remaining texture images are considered for testing purpose (10x 51=510).

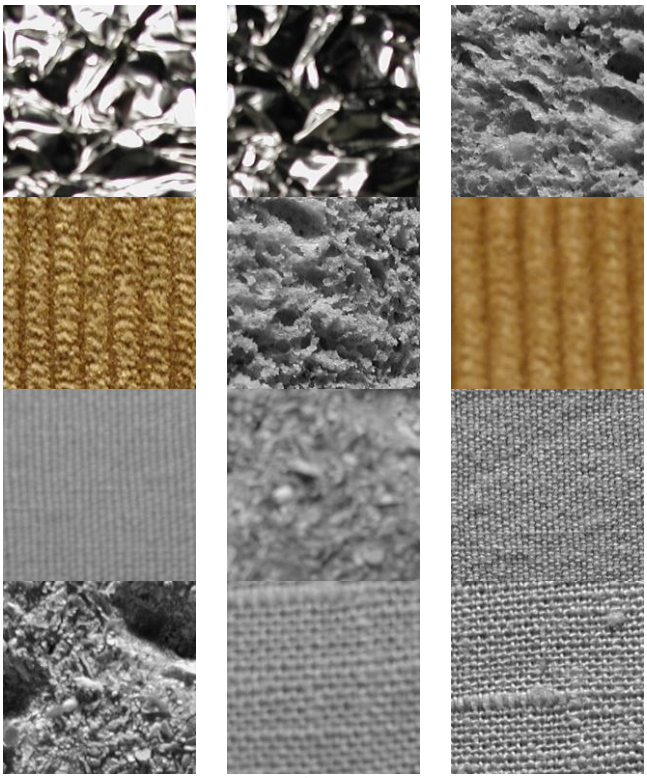

Fig. 9: Sample images of KTU-TIPS texture database.

E. ALOT texture dataset

The ALOT database images are with 384 x 256 dimensions and ALOT database consists of 250 classes of texture images with varied angles and illumination conditions and each class consists of 100 images. This leads to a total of 250 x 100 images. This paper considered 40 images from each class for training (25 x 40=1000) and the remaining 60 images from each class (25 x 60=1500) are considered for testing purpose. The ALOT database images are displayed in Fig. 10.

Fig. 10: ALOT texture database.

The GLCM reflect, degree of correlation between pairs of pixels in different aspects (in terms of homogeneity, uniformity...etc). One of the main factors that affect the discrimination capabilities of GLCM is the separation distance between pixels, i.e. the d value. When you take the distance 1 it leads to reflect the degree of correlation between adjacent pixels (i.e., short range neighbourhood connectivity). While, increasing the distance value leads to reflect the degree of correlation between distant pixels. The present paper initially constructed GLCM on CEWSTM coded image and also on RCEWSTM coded image with d= 1, 2, 3 and 4 and derived five GLCM features on each of the referred database images. For classification purpose this paper computed the average feature value from each distance value and it is given as input to different classifiers. This paper used Naive Bayes classifier, multilayer perceptron (MLP), liblinear and J48 classifiers on WEKA tool for classification purpose.

The proposed CEWSTM and RCEWSTM descriptors have shown high classification rate for d=2, on all four classifiers and on all considered databases and this can be depicted in Fig.11. The multilayer perceptron exhibits a high classification rate for d value=2 on all databases, when compared to other classifiers on the two proposed descriptors (from table 1). For comparison purpose with the other existing descriptors, now onwards the classification rates of multilayer perceptron are quoted for the proposed two descriptors.

Table 1: Average classification rate on different databases using different classifiers for d=2.

Proposed Method	Databases	Naviebayes	Multilayer-perceptron	Ibk	J48
Proposed CEWSTM	Brodtaz	85.23	93.78	89.63	86.32
	ALOT	82.56	89.26	86.21	84.52
	KTH	88.52	94.25	91.42	90.14
	UIUC	87.62	93.29	92.13	89.62
	Outex-TC-12	89.62	95.56	91.99	91.45
Proposed RCEWSTM	Brodtaz	82.14	92.62	86.23	84.63
	ALOT	79.62	86.14	82.45	81.20
	KTH	82.47	92.16	86.85	85.63
	UIUC	83.16	92.14	87.96	86.62
	Outex-TC-12	84.86	94.78	90.45	89.12

Table 2: Classification rate of proposed and existing methods.

Methods	Brodtaz [44]	UIUC[45]	Outex-TC-12 [46]	KTH-TIPS [47]	A LOT [48]
LBP[6]	54.28	56.19	62.86	52.26	64.16
ULBP [42]	40.36	65.19	54.65	40.14	56.24
LTP[12]	57.50	75.88	67.16	56.24	66.18
CLBP_SMC[43]	85.23	90.30	87.64	80.46	89.14
CS-LBP[40]	74.56	74.24	74.64	72.14	70.14
Proposed CEWSTM	93.78	95.56	93.29	89.26	94.25
Proposed RCEWSTM	92.62	94.78	92.14	86.14	92.16

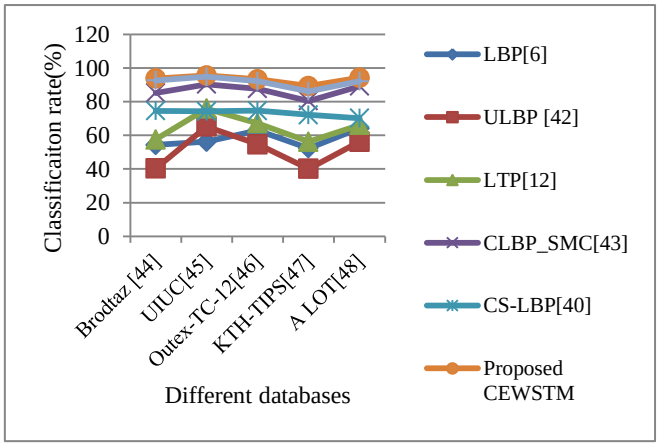

Fig. 11: Comparison graph for existing and proposed methods.

This paper computed the histograms on LBP and LTP and the histograms are used for classification purpose using various classifiers. The histogram size of LBP is 256 and two histograms of sizes 256 each is derived for LTP. These two descriptors are not integrated with GLCM due its high dimensionality i.e. 256 x 256. This paper derived GLCM on ULBP and CS-LBP and computed the five GLCM features. These features are given as inputs to the classifi-

ers and classification is performed. The dimension of "ULBP-GLCM" and "CS-LBP-GLCM" are 59 x 59 and 16 x 16 respectively. The LBP and LTP have exhibited poor performance because of histogram methods. The classification rates of the proposed CEWSTM and RCEWSTM descriptors and the existing descriptors are listed out in table 2 for Brodtaz, UIUC, Outex-TC-12, KTH-TIPS and ALOT databases.

The proposed descriptors have shown a huge improvement over LBP, ULBP, LTP and CS-LBP approaches on all databases. The classification accuracy of the existing methods have shown comparatively less performance on UIUC database due to the scale changes and orientations present in the data base images. The proposed descriptors CEWSTM and RCEWSTM represent both circular and elliptical neighbourhoods. And they have precisely represented both elliptical and circular structural features and due to their low dimensionality they could able to derive statistical features by computing GLCM and thus able to capture more spatial information and sustain scale and orientation changes.

The limitations of the existing texture features LBP, ULBP, CS-LBP and LTP, for texture classification are analysed. LBP, UBLP and LTP differentiate a bright object against a dark background and vice-versa. This differentiation makes the object intra-class variation larger. The CS-LBP though measures the symmetric relations of neighbours but if yields a poor classification rates due to its short code on the other hand LBP, ULBP and LTP when integrated with GLCM produces a huge dimensions and this makes them too complex and not suitable to real time applications. Further all the above descriptors only captures isotropic information and they completely fail in representing anisotropic information, which is also very important in recognizing textures. The proposed CEWSTM and RCEWSTM solve the above problems by deriving the isotropic and anisotropic information on CEN and with a minimum code that represents texture features more precisely. The RCEWSTM maps the CEWSTM code and its complement in the same block to the some value. This causes some local structures to be misrepresented in RCEWSTM and that's RCEWSTM exhibited a low classification rate when compared to CEWSTM. The two new descriptors CEWSTM and RCEWSTM are proposed by analysing the weakness of LBP, ULBP, CS-LBP and LTP. The two proposed descriptor alleviate the problem of existing descriptors of LBP by considering the weighted centre value on CEN.

V. Conclusions

This paper proposed two new local descriptors for a precise texture classification. The two new descriptors are basically extensions to the CS-LBP [40] and CE-LBP. The CS-LBP is proposed in the literature, to reduce the dimensionality aspect of LBP and to measure the relationship between symmetric neighbours of the circular window and thus it only measures the centre symmetric isotropic structural information. The CS-LBP could not yield useful result because of it's too small bit code which ranges from 0 to 15 (4 bit code) and further if has not considered the centre pixel in measuring the symmetric relationship, this makes the CS-LBP as a weak descriptor. The CE-LBP [38] proposed in the literature quantized the circular and elliptical neighbourhood(CEN) with 8-sampling points instead of 12 sampling points, However it is not suitable to derive GLCM features because of its huge dimensions 256 x 256. This paper proposed CEWSTM, a new descriptor that captures both isotropic and anisotropic information without any quantization process, and considers all 12-sampling points of CEN. And it measures the relationship between weighted centre pixel and symmetric pixels of CEN. The proposed CEWSTM recognizes more precise and compact edge information of CEN and its code ranges from 0 to 63 i.e. a 6 bit code. The second descriptor RCEWSTM is more robust and compact than CEWSTM. The RCEWSTM reduces the range of its code from 0 to 31. The GLCM features derived on CEWSTM and RCEWSTM attained a high classification rate when compared to other existing LBP variants. The reason for this is both the descriptors preserves more edge, structural and statistical information of the circular and elliptical neighbourhoods.

References

[1] M. Pietikänen, A. Hadid, G. Zhao, and T. Ahonen, Computer Vision Using Local Binary Patterns. London, U.K.: Springer, 2011.

[2] M. Pietikäinen and G. Zhao, "Two decades of local binary patterns: A survey," in Advances in Independent Component Analysis and Learning Machines. Amsterdam, The Netherlands: Elsevier, 2015.

[3] U. Kandaswamy, S. A. Schuckers, and D. Adjeroh, "Comparison of texture analysis schemes under nonideal conditions," IEEE Trans. Image Process., vol. 20, no. 8, pp. 2260–2275, Aug. 2011.

[4] J. Zhang, M. Marszalek, S. Lazebnik, and C. Schmid, "Local features and kernels for classification of texture and object categories: A comprehensive study," Int. J. Comput. Vis., vol. 73, no. 2, pp. 213–238, Jun. 2007.

[5] S. Brahnam, L. C. Jain, L. Nanni, and A. Lumini, Eds., Local Binary Patterns: New Variants and Applications. London, U.K.: Springer, 2014.

[6] T. Ojala, M. Pietikäinen, and T. Maenpää, "Multiresolution gray-scale and rotation invariant texture classification with local binary patterns," IEEE Trans. Pattern Anal. Mach. Intell., vol. 24, no. 7, pp. 971–987, Jul. 2002.

[7] T. Ahonen, A. Hadid, and M. Pietikäinen, "Face description with local binary patterns: Application to face recognition," IEEE Trans. Pattern Anal. Mach. Intell., vol. 28, no. 12, pp. 2037–2041, Dec. 2006.

[8] G. Zhao and M. Pietikäinen, "Dynamic texture recognition using local binary patterns with an application to facial expressions," IEEE Trans. Pattern Anal. Mach. Intell., vol. 29, no. 6, pp. 915–928, Jun. 2007.

[9] T. Ahonen, J. Matas, C. He, and M. Pietikäinen, "Rotation invariant image description with local binary pattern histogram Fourier features," in Proc. Scandinavian Conf. Image Anal., 2009, pp. 61–70.

[10] L. Liu, L. Zhao, Y. Long, G. Kuang, and P. Fieguth, "Extended local binary patterns for texture classification," Image Vis. Comput., vol. 30, no. 2, pp. 86–99, Feb. 2012.

[11] X. Qi, R. Xiao, C.-G. Li, Y. Qiao, J. Guo, and X. Tang, "Pairwise rotation invariant co-occurrence local binary pattern," IEEE Trans. Pattern Anal. Mach. Intell., vol. 36, no. 11, pp. 2199–2213, Nov. 2014.

[12] X. Tan and B. Triggs, "Enhanced local texture feature sets for face recognition under difficult lighting conditions," IEEE Trans. Image Process., vol. 19, no. 6, pp. 1635–1650, Jun. 2010.

[13] Y. Guo, G. Zhao, and M. Pietikäinen, "Discriminative features for texture description," Pattern Recognit., vol. 45, no. 10, pp. 3834–3843, Oct. 2012.

[14] L. Liu, L. Zhao, Y. Long, G. Kuang, and P. Fieguth, "Extended local binary patterns for texture classification," Image Vis. Comput., vol. 30, no. 2, pp. 86–99, Feb. 2012.

[15] Z. Guo, L. Zhang, and D. Zhang, "A completed modeling of local binary pattern operator for texture classification," IEEE Trans. Image Process., vol. 19, no. 6, pp. 1657–1663, Jun. 2010

[16] X. Qi, R. Xiao, C.-G. Li, Y. Qiao, J. Guo, and X. Tang, "Pairwise rotation invariant co-occurrence local binary pattern," IEEE Trans. Pattern Anal. Mach. Intell., vol. 36, no. 11, pp. 2199–2213, Nov. 2014.

[17] S. Liao, M. W. K. Law, and A. Chung, "Dominant local binary patterns for texture classification," IEEE Trans. Image Process., vol. 18, no. 5, pp. 1107–1118, May 2009.

[18] V. Ojansivu, E. Rahtu, and J. Heikkilä, "Rotation invariant local phase quantization for blur insensitive texture analysis," in Proc. IEEE Int. Conf. Pattern Recognit. (ICPR), Dec. 2008, pp. 1–4.

[19] D. K. Iakovidis, E. G. Keramidas, and D. Maroulis, "Fuzzy local binary patterns for ultrasound texture characterization," in Image Analysis and Recognition (Lecture Notes in Computer Science), A. Campilho and M. Kamel, Eds. Berlin, Germany: Springer, 2008, pp. 750–759.

[20] J. Chen, V. Kellokumpu, G. Zhao, and M. Pietikänen, "RLBP: Robust local binary pattern," in Proc. Brit. Vis. Conf. Comput. Vis. (BMVC), 2013, pp. 1–10.

[21] Hafiane, G. Seetharaman, and B. Zavidovique, "Median binary pattern for textures classification," in Proc. 4th Int. Conf. Image Anal. Recognit., 2007, pp. 387–398.

[22] Fathi and A. R. Naghsh-Nilchi, "Noise tolerant local binary pattern operator for efficient texture analysis," Pattern Recognit. Lett., vol. 33, no. 9, pp. 1093–1100, Jul. 2012.
[23] J. Ren, X. Jiang, and J. Yuan, "Noise-resistant local binary pattern with an embedded error-correction mechanism," IEEE Trans. Image Process., vol. 22, no. 10, pp. 4049–4060, Oct. 2013
[24] T.Ahonen,A. Hadid,M. Pietikäinen, Face recognition with local binary patterns, :Proceedings of Eighth European Conference on Computer Vision, 2004,pp.469–481.
[25] Z. Lei, S.Liao, M.Pietikäinen, S.Z.Li, Face recognition by exploring information jointly in space, scale and orientation, IEEE Trans. ImageProcess.20(1)(2011) 247–256.
[26] T.Jabid, M.H.Kabir, O.Chae, Local directional pattern(LDP)-a robust image descriptor for Object Recognition, in: Proceedings of 7th IEEE International Conference on Advanced Video and Signal Based Surveillance,2010,pp.482–487
[27] Lakhdar Belhallouche ,, Kamel Belloulata, Kidiyo Kpalma , A New Approach to Region Based Image Retrieval using Shape Adaptive Discrete Wavelet Transform, I.J. Image, Graphics and Signal Processing, 2016, 1, 1-14.
[28] Pranoti P. Mane , Narendra G. Bawane , Image Retrieval by Utilizing Structural Connections within an Image , I.J. Image, Graphics and Signal Processing, 2016, 1, 68-74.
[29] K. Prasanthi Jasmine1 ; P. Rajesh Kumar2 , Color and Rotated M-Band Dual Tree Complex Wavelet Transform Features for Image RetrievalM. I.J. Image, Graphics and Signal Processing, 2014, 9, 1-10.
[30] X. Huang, S.Z. Li, Y. Wang, Shape localization based on statistical method using extended local binary patterns, in: Proc. Inter. Conf. Image and Graphics, Beijing, China, 2004, pp. 184–187.
[31] Ding, C. Xu, and D. Tao, "Multi-task pose-invariant face recognition," IEEE Trans. Image Process., vol. 24, no. 3, pp. 980–993, Mar. 2015.
[32] V. Vijaya Kumar, K. Srinivasa Reddy, V. Venkata Krishna "Face Recognition Using Prominent LBP Model", International Journal of Applied Engineering Research , Vol. 10, Iss. 2, 2015, pp. 4373-4384, ISSN: 0973-4562
[33] M. Heikkila, M. Pietikainen, A texture based method for modeling the background and detecting moving objects, IEEE Trans. Pattern Anal. Mach.Intell. 28 (4) (2006) 657–662.
[34] Paweł Tarnowski, Marcin Kołodziej, Andrzej Majkowski, Remigiusz J. Rak, Emotion recognition using facial expressions, Procedia Computer Science 108C (2017) 1175–1184.
[35] Guo Xianhai, Study of Emotion Recognition Based on Electrocardiogram and RBF neural network, Advanced in Control Engineering and Information Science, Procedia Engineering 15 (2011) 2408 – 2412.
[36] M. Heikkila, M. Pietikainen, C. Schmid, Description of interest regions with local binary patterns, Pattern Recogn. 42 (2009) 425–436.
[37] M. Li, R.C. Staunton, Optimum Gabor filter design and local binary patterns for texture segmentation, Elsevie J. Pattern Recogn. 29 (2008) 664–672.
[38] K. Subba Reddy, V. Vijaya Kumar, A.P. Siva Kumar, Classification of Textures Using a New Descriptor Circular and EllipticalLBP (CE-ELBP), International Journal of Applied Engineering Research ISSN 0973-4562 Volume 12, Number 19 (2017) pp. 8844-8853
[39] K. Subba Reddy, V. Vijaya Kumar, A.P. Siva Kumar, Cross Diagonal Circular and Elliptical Texture Matrix For Efficient Texture Classification, Journal of Advanced Research in Dynamical and Control Systems, (Accepted).
[40] Heikkilä, M., Pietikäinen, M., Schmid, C.: Description of interest regions with local binary patterns. Pattern Recognit. 42(3), 425–436 (2009).
[41] Haralick RM , Shanmugan K and Dinstein I, "Textural features for image classification", IEEE Trans. Sysr., Man., Cybern., Vol. SMC-3, no. 6, pp. 610-621, 1973.
[42] Zhao G, Ahonen T, Matas J, Pietikainen M (2011) Rotation-invariant image and video description with local binary pattern features. IEEE Transactions on Image Processing 21(4): 1465–1477
[43] Marko Heikkil¨a, Matti Pietik¨ainen, and Cordelia Schmid, Description of Interest Regions with Center-Symmetric Local Binary Patterns, P. Kalra and S. Peleg (Eds.): ICVGIP 2006, LNCS 4338, pp. 58–69, 2006
[44] P. Brodatz, Textures: A Photographic Album for Artists and Designers. New York, NY, USA: Dover, 1996.
[45] S. Lazebnik, C. Schmid, and J. Ponce, "A sparse texture representation using local affine regions," IEEE Trans. Pattern Anal. Mach. Intell.,vol. 27, no. 8, pp. 1265–1278, Aug. 2005
[46] http://www.outex.oulu.fi/index.php?page=image_databaseS.
[47] E. Hayman, B. Caputo, M. Fritz, and J. Eklundh, "On the significance of real-world conditions for material classification," in European Conference on Computer Vision (ECCV), 2004, pp. 253–266
[48] G. J. Burghouts and J.-M. Geusebroek, "Material-specific adaptation of color invariant features," Pattern Recognit. Lett., vol. 30, no. 3,pp. 306–313, Feb. 2009.